Silja Holopainen, Farshid Manoocheri, and Erkki Ikonen. 2009. Non-Lambertian behaviour of fluorescence emission from solid amorphous material. Metrologia, volume 46, number 4, pages S197-S201.

http://www.iop.org/journals/met
http://stacks.iop.org/met/46/S197

x0000 - xx xxxx 2009 metrologia

Non-Lambertian behaviour of fluorescence emission from solid amorphous material

Silja Holopainen, Farshid Manoocheri and Erkki Ikonen

Abstract. The commonly made assumption of Lambertian behaviour of fluorescence emission has been studied in solid amorphous material. A goniofluorometer capable of measurements in measurement geometries from 0 : 10 to 0 : 85 has been used for this purpose. The measurements indicate that the fluorescence emission from solid amorphous material is clearly non-Lambertian.

1. Introduction

Fluorescence is a widely used phenomenon in various scientific and industrial applications. Fluorescence measurements are vitally important when determining the colour and appearance of e.g. paper, textile, and plastic products. The whiteness of normal copying paper is also commonly enhanced by adding a fluorescent brightening agent that excites in the UV region and emits in the blue part of the visible spectrum which compensates for the yellowness of the paper.

The colour properties of an object depend on the illumination, the observer and the object. The colour of the object can be defined by its tristimulus values which are dependent on all three factors. If an object's source independent bispectral radiance factor data, namely the Donaldson radiance factor data [1], are known, the tristimulus values can be calculated for the desired illumination and observer. The bispectral radiance factor data comprise the reflection radiance factors and the bispectral luminescent radiance factors.

Most measurement facilities capable of absolute fluorescence measurements apply a fixed measurement geometry [2–4] and rely on the assumption of Lambertian emission of fluorescence from liquids and solid amorphous material. The angular behaviour of fluorescence has been extensively studied from solid crystalline materials in the context of studying the orientation of the fluorophores [5–8]. However, to our knowledge it has not been studied from solid amorphous material.

We have developed a goniofluorometer capable of absolute measurements of the bispectral luminescent radiance factor from solid samples in various measurement geometries [9]. In this paper, we present bispectral luminescent radiance factors measured as a function of the viewing angle. These measurement results challenge the common assumption of Lambertian behaviour of fluorescence emission from solid amorphous material.

The goniofluorometer can also be used to measure fluorescence quantum yield, the number of emitted photons relative to the number of absorbed photons. Several methods exist for measuring the absolute fluorescence quantum yield including e.g. methods based on measuring the absorbed excitation flux and the emitted fluorescence flux using an integrating sphere [10–13]. Some other existing methods which are mostly applicable to solutions are calorimetric methods which determine the fluorescence quantum yield by comparison of the heating rates of the measured solvent and an inert reference absorber [14] and thermal lensing methods which determine the non-radiative decay of the measured solution through measuring the change in intensity of a small part of the transmitted radiation due to thermal expansion in the solution [15, 16]. In the appendix, available from the online version of this journal, we present the theory and mathematics for determining the absolute fluorescence quantum yield from solid samples based on goniometric measurements of the emitted and reflected spectra.

2. Instruments and methods

The goniofluorometer is presented in figure 1 and a detailed description is given in reference [9]. The de-

Silja Holopainen, Farshid Manoocheri and Erkki Ikonen: Metrology Research Institute, Helsinki University of Technology (TKK), P. O. Box 3000, FI-02015 TKK, Finland
Centre for Metrology and Accreditation (MIKES), P.O. Box 9, FI-02151 Espoo, Finland

vice uses two optional light sources; a Xenon lamp up to 450 nm and a halogen-tungsten quartz lamp that can be used above 400 nm. The excitation wavelength selection is provided by a double monochromator and some additional optics is employed to polarize, guide and collimate the excitation radiation on to the sample. A beam splitter directs a small fraction of the incident radiation to a monitor detector which is used to minimize the effect of possible fluctuations in the incident beam power.

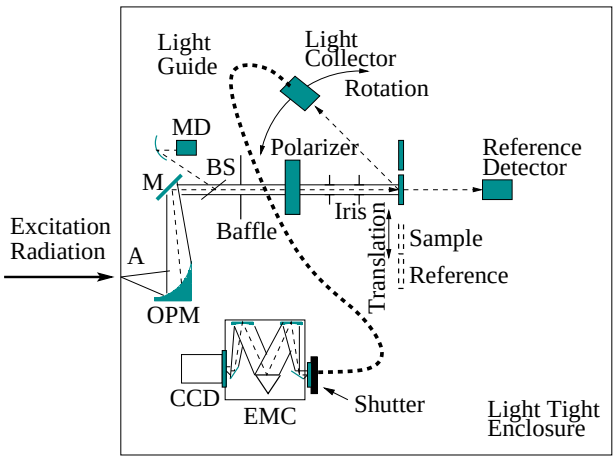

Figure 1. The goniofluorometer: A, aperture; OPM, off-axis parabolic mirror; M, flat mirror; BS, beam splitter; MD, monitor detector; EMC, emission monochromator; and CCD, charge-coupled device.

The sample holder system comprises two sample holders; one for the fluorescent sample and one for a non-fluorescent reflectance standard. The diameter of the incident beam on the sample is 15 mm. The selection between the samples is provided by a motorized linear translator. The emitted and reflected flux are collected by a light collector (aperture + lens) and focused on the input of a fibre bundle which is used to guide the light into the emission spectrometer (EMS). The EMS comprises a monochromator and a CCD detector. The light collector is mounted on a cantilever which lies on a high-accuracy turntable providing viewing angles from 10° to 90° relative to the incident beam. The surfaces of the fluorescent sample and the non-fluorescent reference standard are aligned to lie on the rotation axis of the turntable according to reference [9]. The incident angle is adjusted with the help of a mirror in the sample (reference) position. These procedures ensure the same measurement geometry for the sample and the reference.

The emission monochromator (EMC) [17] employed in these measurements is different from that described in reference [9]. The new monochromator has three gratings and a filter wheel which is also used as a shutter. In the measurements, two ruled gratings with 1200 lines/mm (dispersion 2.4 nm/mm) and blaze wavelengths at 300 nm and 500 nm are used. The new EMC is superior to the old EMC in terms of wavelength accuracy and repeatability and has a flat focal plane contrary to the spherical one in the old EMC. The change of the emission monochromator has considerably reduced uncertainties related to the wavelength scale and stray light.

The wavelength calibration of both the excitation monochromator and the EMC-CCD combination have been done against mercury spectral lines. This calibration is repeated if needed. The need for wavelength calibration can be monitored by monitoring a possible shift of the non-fluorescent reference standard reflection peak on the CCD. The monitor detector has been checked by measuring its drift with time when illuminated by the relatively stable halogen-tungsten source. The performance of the detector can be followed from the measurement signals of the monitor during each measurement. The spectral responsivity of the monitor detector is not needed since it is used only to measure the relative change in the excitation beam power within one wavelength. The spectral responsivity calibration of the EMS with the new EMC, including the light collector and the fibre, has been performed several times within two days. The last calibration was performed just before the measurements reported in this paper and the change in the calibration within this time is treated as an uncertainty component. The responsivity calibration is repeated, if the measurement system has been shut down for several days. This interval may be lengthened in the future, if no significant changes are observed.

In order to obtain the fluorescence signal per unit wavelength interval for the bispectral luminescent radiance factor calculation (see also (1)), the EMS dispersion (nm/pixel) must be known. The theoretical value can be calculated from the specified EMC dispersion (nm/mm) and its uncertainty has been estimated by measuring two mercury lines simultaneously on the CCD and calculating the EMS dispersion (nm/pixel) from this measurement. Then this measured value has been used to correct the theoretical value. The standard uncertainty of the dispersion is taken as the magnitude of the correction. The effect of this uncertainty component on the bispectral luminescent radiance factor has been estimated by calculating bispectral luminescent radiance factors using different dispersions based on the uncertainty of the dispersion.

Another uncertainty component arises from the broadening of the fluorescence spectrum due to emission and excitation monochromator slit scattering functions. The measured width of the reflection spec-

trum at the emission monochromator is 3.9 nm (full width at half maximum). The measured fluorescence spectrum is a convolution of the true fluorescence spectrum without broadening and the slit scattering function of the monochromators obtained from the reflection measurement. Using a simple model that the fluorescence spectrum and the reflected signal are of Gaussian shape, we have calculated an estimate for the width of the true fluorescence spectrum and the associated relative uncertainty due to the broadening.

We have also investicated a possible shift in the fluorescence spectrum due to excitation wavelength by measuring the fluorescence spectrum using two excitation wavelengths, namely 350 nm and 380 nm. We found that the effect of the excitation wavelength is negligible and the position and shape of the emission spectrum remain the same. This is also true when investigating the shape of the fluorescence spectrum and the width of the reflection peak as a function of the viewing angle. When reflectance is measured, the whole reflected peak is viewed by the CCD and the whole peak is used in the calculation of the bispectral luminescent radiance factor and therefore the integrated reflection signal is not affected by the slit width of the excitation or the emission monochromator

The measurement procedure of the goniofluorometer is such that at each measurement angle and excitation wavelength reflectance is measured from both the fluorescent sample and the non-fluorescent reference. The monitor signal is recorded for both measurements. Then the fluorescent emission is measured from the sample at each required emission monochromator position and the monitor signal is recorded. This procedure is repeated for all desired viewing angles and both orthogonal polarization states of the incident radiation. All measured signals are corrected by the monitor readings in order to avoid errors due to fluctuations in the incident beam. If the excitation and emission spectra of the measured sample overlap, the overlapping part of the emission can be estimated by extrapolation. The bispectral luminescent radiance factor is calculated from the measurement results by

$$\beta_{L\mu}(\lambda,\theta) = \frac{i_s(\mu,\lambda,\theta)}{I_{std}(\mu,\theta)}\beta_{std}(\mu,\theta), \qquad (1)$$

where $i_s(\mu,\lambda,\theta)$ is the fluorescent signal in direction θ relative to the sample normal per unit wavelength interval at wavelength λ when irradiated at wavelength μ, $I_{std}(\mu,\theta)$ is the signal from the reference standard and $\beta_{std}(\mu,\theta)$ is the radiance factor of the reference. The signals are corrected for instrumental errors, such as EMS responsivity, according to reference [9] and the monitor correction is applied.

3. Measurement results and uncertainty

Figure 2 presents bispectral luminescent radiance factors, $\beta_{L\mu}(\lambda,\theta)$, of a Spectralon based sample SFS-461-020 [18] for four emission wavelengths as a function of the viewing angle. The incident angle is near normal and the excitation wavelength is 350 nm. The bispectral luminescent radiance factors have been calculated with (1). The radiance factors of the reference have been measured with our gonioreflectometer [19–21]. The reference standard is also a Spectralon sample [18] so that its material properties are expected to be similar to the fluorescence sample. A Spectralon standard was chosen in order to have good comparability between the sample and the reference. The bispectral luminescent radiance factors from figure 2 are presented in figure 3 together with the reflection radiance factors of the sample at 350 nm and 380 nm. In figure 3, all values have been scaled to unity at 10° in order to illustrate their relative angular dependence. The error bars in the figures indicate uncertainties with coverage factor $k = 2$. In figure 3 error bars have been omitted for all but one emission and one reflectance wavelength for clarity.

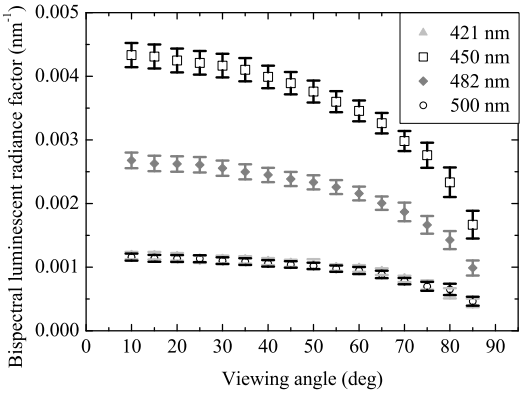

Figure 2. Bispectral luminescent radiance factors of SFS-461-020 for emission wavelengths 421, 450, 482 and 500 nm. The data at 421 nm and 500 nm are almost coincident and 450 nm is close to the emission maximum. The excitation wavelength is $\mu = 350$ nm.

The fluorescence emission has been measured down to 370 nm where the emission is practically non-existent and the emission spectrometer conveniently misses the reflected radiation at 350 nm. Reliably measurable fluorescence is detected only above 400 nm. Also according to the manufacturer, the relative emission spectrum of SFS-461-020 is practically zero below 400 nm [18].

The sample was measured also 90° rotated in

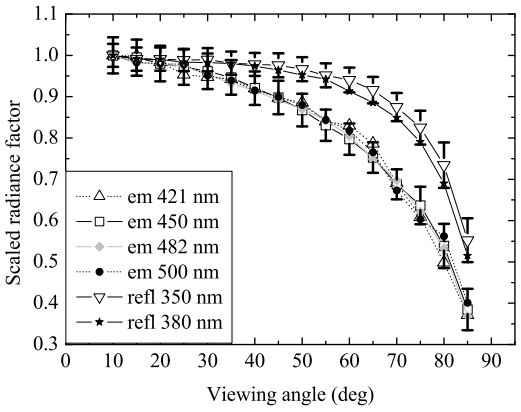

Figure 3. Bispectral luminescent radiance factors (em 421 nm, em 450 nm, em 482 nm and em 500 nm) and reflection radiance factors (refl 350 nm and refl 380 nm) scaled to unity at 10° viewing angle.

order to confirm cylindrical symmetry. The measured bispectral luminescent radiance factors were well within the uncertainties of figure 2 except for viewing angles 75° and 80°. Monitor readings during the measurement of those angles indicate that the discrepancies have been caused by light source instability when measuring at p-polarization (measurements at s-polarization agreed well between the 90° rotated and the not rotated sample for all viewing angles). Although the monitor correction is applied to all measurement signals, due to the slight delay between the monitor reading and the CCD reading ($\sim 1-3$ s), very sudden steep jumps in the output of the Xenon source may not be properly corrected by the monitor detector. However, in our experience this kind of changes in source intensity are rare.

The uncertainty budget is presented in table 1 for the bispectral luminescent radiance factor at 0 : 45 measurement geometry and 450 nm emission wavelength. The largest uncertainty component is related to the emission spectrometer dispersion (nm/pixel) and it is discussed in section 2.. The uncertainty of the radiance factor of the reference is larger than that reported in [21] due to the use of a less stable sample holder. In the fluorescence measurements two sample holders are needed to hold both the measured sample and the non-fluorescent reference standard. The holder used for the reference standard in the fluorescence measurements has more uncertainty in the aperture-to-sample distance and in the illumination and viewing angles than the holder used in the reflectance measurements. In the fluorescence measurements the better holder is employed by the fluorescence sample.

Table 1. Relative standard uncertainties in the bispectral luminescent radiance factors in 0 : 45 geometry at the emission wavelength of 450 nm. The numbers in parenthesis give the standard uncertainty of the component. The first three components are of type A and the rest are of type B. All uncertainties have been derived according to reference [22].

Source of uncertainty	Rel. Uncert. in $\beta_{L\mu}(\lambda,\theta) \times 100$
Measurement repeatability	0.28
Random noise	0.71
EMS calib. repeatability	0.20
CCD response uniform.	1.0
CCD linearity	0.10
Ref. det. responsivity	0.30
Illum. and viewing angles (0.2°)	0.12
Radiance factor of reference	1.1
Stray light	0.57
Wavelength (ex.) (0.15 nm)	0.10
Wavelength (em.) (0.17 nm)	0.2
Slit scattering functions	0.2
EMS dispersion	1.7
Combined stand. uncert.	2.5

4. Discussion

The angular behaviour of the fluorescence emission observed in figures 2 and 3 is validated through comparison measurements [21] performed between the TKK (Helsinki University of Technology) [19,20] and PTB (Physikalish-Technische Bundesanstalt) [23] gonioreflectometers. The validation could not be made between fluorometers, because to our knowledge there are no other fluorometers capable of angular measurements of the bispectral luminescent radiance factor. In this comparison of the 0 : 45 radiance factor and goniometrically determined diffuse reflectance, the angular behaviour of both gonioreflectometers over viewing angles from 10° to 85° was found to be very similar. Figure 4 illustrates the angular behaviour of both gonioreflectometers. The measured sample is a white sample made of sintered PTFE (polytetrafluoroethylene). The measurements have been performed at 500 nm. The radiance factors of the non-fluorescent reference, used in the fluorescence measurements, have been measured with the TKK gonioreflectometer. The core element in both the gonioreflectometer [19,20] and the goniofluorometer [9] is the same high-accuracy turntable providing the viewing angles. The additional uncertainty components introduced in the fluorescence measurements are, apart from the increased uncertainty of

the reference standard viewing angle and sample-to-aperture distance, related to the properties of the emission spectrometer and are not angle dependent. The standard uncertainty in the viewing angle and in the distance setting is constant for all angles and its effect on the bispectral luminescent radiance factor can be dealt with by increasing the uncertainty of the radiance factor of the reference as explained in section 3.. The uncertainty in the radiance factor can be easily calculated for each angle and has been treated accordingly.

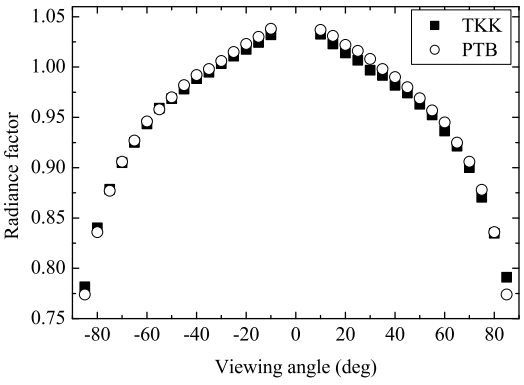

Figure 4. Radiance factors measured in-plane as a function of viewing angle at 500 nm. The measured sample is a white standard made of sintered PTFE.

In solid crystalline material, the fluorophor has a particular orientation which contributes to the observed angular profile of the emission, but in an amorphous material the fluorophor orientation could be expected to be random and therefore not contribute to the angular pattern of the emission. However, figure 2 indicates a clear deviation of the fluorescence emission from Lambertian behaviour measured from an amorphous fluorescence standard. If the emission were Lambertian, the bispectral luminescent radiance factors would be constant with respect to the viewing angle. Moreover, figure 3 shows how the angular profile of the fluorescence emission is the same for all emission wavelengths, but diverges clearly from the angular profile of the reflectance. This suggests that the fluorophor orientation may not be as random as assumed or there may be scattering or other effects on the surface of the sample which significantly contribute to the observed geometrical distribution of the fluorescence emission. Also, especially at oblique angles some of the emitted radiation may be absorbed before it can escape from the sample and thus reduce the observed emission at these angles. These phenomena are always present when measuring solid samples and contribute to the reflection pattern of both the sample and reference standard as well. In spite of that, the angular behaviour of emission is clearly not very tightly tied to the angular behaviour of reflectance. The deviation from Lambertian behaviour is so large ($\sim$ 60 % between viewing angles 10° and 85° and $\sim$ 10 % between 10° and 45°) that illumination and viewing angles should be carefully considered when measuring and calibrating the radiance factors of fluorescent samples.

In conclusion, the measurement results presented in this paper show that the bispectral luminescent radiance factors of solid amorphous samples can not be considered independent of the viewing angle.

Acknowledgements

The authors would like to thank Jonna Paatelma for her help with the measurement programs and characterization of the emission monochromator. The authors also give thanks to Dr. Andreas Höpe and Kai-Olaf Hauer for the PTB data in figure 4. Silja Holopainen appreciates the support of the Foundation of Technology – TES and the Finnish Foundation for Economic and Technology Sciences – KAUTE.

References

1. Donaldson R., *British Journal of Applied Physics*, 1954, **5**, 210-214.
2. Zwinkels J. C. and Gauthier F., *Analytica Chimica Acta*, 1999, **380**, 193-209.
3. Monte C., Pilz W., and Resch-Genger U., *Proc. SPIE*, 2005, **5880**, 1-10.
4. DeRose P. C., Early E. A., and Kramer G. W., *Review of Scientific Instruments*, 2007, **78**, 033107.
5. Thompson N. L., McConnell H. M., and Burghardt T. P., *Biophys. J.*, 1984, **46**, 739-747.
6. Edmiston P. L., Lee J. E., Wood L. L., Saavedra S. S., *J. Phys. Chem.*, 1996, **100**, 775-784.
7. Lambacher A. and Fromherz P., *J. Phys. Chem.*, 2001, **105**, 343-346.
8. Barritault P., Gétin S., Chaton P., Vinet F., and Fouqué B., *Applied Optics*, 2002, **41**, 4732-4738.
9. Holopainen S., Manoocheri F., and Ikonen E., *Applied Optics*, 2008, **47**, 835-842.
10. Greenham N. C., Samuel I. D. W., Hayes G. R., Phillips R. T., Kessener Y. A. R. R., Moratti S. C., Holmes A. B., Friend R. H., *Chemical Physics Letters*, 1995, **241**, 89-96.
11. de Mello J. C., Wittmann H. F., and Friend R. H., *Advanced Materials*, 1997, **9**, 230-232.
12. Porrés L., Holland A., Pålsson L.-O., Monkman A. P., Kemp C., and Beeby A., *Journal of Fluorescence*, 2006, **16**, 267-272.
13. Gaigalas A. K. and Wang L., *Journal of Research of the National Institute of Standards and Technology*, 2008, **113**, 17-28.
14. Olmsted J., *Journal of Physical Chemistry*, 1979, **83**, 2581-2584.
15. Brannon J. H. and Magde D., *Journal of Physical Chemistry*, 1978, **82**, 705-709.

16. Magde D., Wong R. and Seybold P. G., *Photochemistry and Photobiology*, 2002, **75**, 327-334.
17. ANDOR Shamrock SR-303i, Andor Technology, Ltd., Belfast, Ireland.
18. Spectralon Fluorescence Standards, Labsphere, N.H., USA.
19. Nevas S., Manoocheri F., and Ikonen E., *Applied Optics*, 2004, **43**, 6391-6399.
20. Holopainen S., Manoocheri F., Nevas S., and Ikonen E., *Metrologia*, 2007, **44**, 167-170.
21. Holopainen S., Manoocheri F., Ikonen E., Hauer K.-O., and Höpe A., Comparison measurements of 0 : 45 radiance factor and goniometrically determined diffuse reflectance, *in preparation*.
22. Guide to the Expression of Uncertainty in Measurement, ISO 1992, 1st ed., 91 p.
23. Hünerhoff D., Grusemann U., and Höpe A., *Metrologia*, 2006, **43**, S11-S16.

Received on xx xxxx 2009.

Appendix: Fluorescence quantum yield

The fluorescence quantum yield, defined as the number of emitted photons divided by the number of absorbed photons, can be calculated from the measurement results of the goniofluorometer in the following way. Assuming that the sample is thick enough and no transmission occurs, the number of absorbed photons, n_a, can be obtained as the number of incident photons, n_i, minus the number of reflected photons, n_r. For cylindrical symmetry, the hemispherical reflectance factor, $R(\mu)$, of the fluorescent sample can be calculated by integration over polar angles

$$R(\mu) = \int_0^{\frac{\pi}{2}} \beta_r(\mu,\theta)\sin(2\theta)\,d\theta = \frac{n_r(\mu)}{n_{r,prd}(\mu)}, \quad \text{(A1)}$$

where $\beta_r(\mu,\theta)$ is the reflection radiance factor of the fluorescent sample when irradiated at wavelength μ and viewed at angle θ relative to the sample normal and $n_{r,prd}(\mu)$ is the total number of photons reflected by a perfect diffuser. According to the definition, $n_{r,prd}(\mu)$ is equal to $n_i(\mu)$.

The reflection radiance factor can be calculated by

$$\beta_r(\mu,\theta) = \frac{I_s(\mu,\theta)}{I_{std}(\mu,\theta)}\beta_{std}(\mu,\theta), \quad \text{(A2)}$$

where $\beta_{std}(\mu,\theta)$ is the radiance factor of a non-fluorescent reflectance standard and $I_s(\mu,\theta)$ and $I_{std}(\mu,\theta)$ are the measured signals from the fluorescent sample and the reflectance standard, respectively. The number of absorbed photons is $n_a(\mu) = [1-R(\mu)]\cdot n_i(\mu)$ and with (A1) and (A2) it becomes

$$n_a(\mu) = n_i(\mu)\int_0^{\frac{\pi}{2}} \sin(2\theta)[1-\frac{I_s(\mu,\theta)}{I_{std}(\mu,\theta)}\beta_{std}(\mu,\theta)]\,d\theta. \quad \text{(A3)}$$

In order to calculate the total number of photons emitted by the sample at wavelength λ when irradiated at wavelength μ, $n_e(\mu,\lambda)$, we need to determine the hemispherical fluorescence reflection factor of the sample, $R_e(\mu,\lambda)$. This can be calculated with (A1) by replacing $R(\mu)$ with $R_e(\mu,\lambda)$ and the reflection radiance factor, $\beta_r(\mu,\theta)$, with the bispectral luminescent radiance factor, $\beta_{L\mu}(\lambda,\theta)$. The latter can be calculated by

$$\beta_{L\mu}(\lambda,\theta) = \frac{i_s(\mu,\lambda,\theta)}{I_{std}(\mu,\theta)}\beta_{std}(\mu,\theta), \quad \text{(A4)}$$

where $i_s(\mu,\lambda,\theta)$ is the fluorescent signal per unit wavelength interval at wavelength λ when irradiated at wavelength μ. The signals are corrected for instrumental errors, such as EMS responsivity, according to reference [9]. The hemispherical fluorescence reflection factor can also be written as

$$R_e(\mu,\lambda) = \frac{E_s(\mu,\lambda)}{E_{prd}(\mu)} = \frac{n_e(\mu,\lambda)}{n_{r,prd}(\mu)}\cdot\frac{\mu}{\lambda}, \quad \text{(A5)}$$

where $E_s(\mu,\lambda)$ and $E_{prd}(\mu)$ are the energies emitted and reflected by the fluorescent sample and a perfect diffuser, respectively, and equation $E(\lambda) = hc/\lambda$ has been used for the energy of a photon. The total number of photons emitted by the sample when irradiated at wavelength μ can be obtained from (A5) by integration over all emission wavelengths λ

$$n_e(\mu) = \frac{n_i(\mu)}{\mu}\int \lambda R_e(\mu,\lambda)\,d\lambda, \quad \text{(A6)}$$

where $n_i(\mu) = n_{r,prd}(\mu)$. The spectral fluorescence quantum yield, $Q(\mu)$, can be calculated by dividing (A6) by (A3) and using (A1) and (A4) to derive $R_e(\mu,\lambda)$,

$$Q(\mu) = \frac{\int_0^{\pi/2}\left[\beta_{std}(\mu,\theta)\sin(2\theta)\int\lambda\frac{i_s(\mu,\lambda,\theta)}{I_{std}(\mu,\theta)}d\lambda\right]d\theta}{\mu\int_0^{\pi/2}\sin(2\theta)\left[1-\frac{I_s(\mu,\theta)}{I_{std}(\mu,\theta)}\beta_{std}(\mu,\theta)\right]d\theta}, \quad \text{(A7)}$$

where the signals and radiance factors are all functions of μ and θ. For the studied cylindrical symmetry, it is enough to determine the reflected and emitted signals from the sample and reference over polar angles from 0° to 90° relative to the sample normal.

Numerical values of the fluorescence quantum yield determined using the method derived above are not given, because the method has not been properly validated. The validation is planned to be carried out in the near future.